OENO One
vine & wine

DOI: https://doi.org/10.20870/oeno-one.2025.59.1.8244

OPEN ACCESS

ORIGINAL RESEARCH ARTICLES

Comparative genomics of *Rpv3*, a multiallelic downy mildew resistance locus in grapevine (*Vitis* sp.)

Dustin G. Wilkerson[1], Cheng Zou[1], Qi Sun[1], Qandeela Nigar[2,3], Manon Paineau[4], Dario Cantu[4], Chin-Feng Hwang[5], and Lance Cadle-Davidson[2,6*]

[1] Institute of Biotechnology, Cornell University, Ithaca, NY, United States
[2] School of Integrative Plant Sciences, Cornell University, Geneva, NY, United States
[3] Department of Plant Breeding and Genetics, Arid Agriculture University, Rawalpini, Pakistan
[4] Department of Viticulture and Enology, University of California–Davis, Davis, CA, United States
[5] State Fruit Experiment Station at Mountain Grove Campus, Missouri State University, Springfield, MO, United States
[6] USDA-ARS, Grape Genetics Research Unit, Geneva, NY, United States

Article number: 8244

*correspondence:
lance.cadledavidson@usda.gov

Associate editor:
Gabriella De Lorenzis

Received:
30 July 2024

Accepted:
28 February 2025

Published:
11 March 2025

This article is published under the **Creative Commons licence** (CC BY 4.0).

Use of all or part of the content of this article must mention the authors, the year of publication, the title, the name of the journal, the volume, the pages and the DOI in compliance with the information given above.

ABSTRACT

Grapevine downy mildew, caused by the oomycete pathogen *Plasmopara viticola,* can lead to economically significant losses in humid climates. An ever-growing catalog of loci for resistance to *P. viticola* is available to breeders, including *Rpv3* on the lower arm of chromosome 18. Widely used in French-American cultivars, *Rpv3* is a complex TIR-NBS-LRR locus for which associated SSR markers have provided evidence of multiple alleles with varying degrees of resistance. However, SSRs lack the resolution to detect nuances between alleles and fully characterize the locus. PacBio long-read sequencing enables phased assembly of highly repetitive gene cluster regions, allowing for high resolution comparison among predicted alleles. *Rpv3* haplotypes of eight *Vitis* genomes ('Catawba', 'Chambourcin', 'Concord', 'Horizon', MN1264, 'Norton', NY84.0101.03, and PN40024) were compared to identify differences in gene structure among *Rpv3.1*, *Rpv3.2*, *Rpv3.3*, co-located *Rpv27*, and susceptible SSR haplotypes. This region was extracted from each haplotype as delimited by their flanking SSR markers and ranged in length from 0.8 to 1.7 Mb. While there was strong consistency in gene structure within *Rpv3.1*, both *Rpv3.2* and *Rpv3.3* showed evidence of divergence between haplotypes. In addition to local alignments, the candidate genes identified in *Rpv3.1* were tested for copy number and functional variation across haplotypes. The candidate gene region ranged in length from 85.3–220 kb from SSR UDV737. While the structure of this region and the *TNL* gene sequences were largely consistent within *Rpv3.1* and *Rpv3.2,* the structure was variable among *Rpv3.3* individuals. In spite of this structural variation among the *Rpv3.3* SSR haplotype, their *TNL* gene sequences had strong similarity to *Rpv27*. The variation in gene structure shown in this study underscores the need for the refinement of allele naming, high-quality genome assemblies, as well as more informative, higher resolution marker systems for marker-assisted selection to improve resistance to grapevine downy mildew.

KEYWORDS: *Vitis vinifera*, *Vitis labrusca*, *Rpv3*, *Rpv27*, grapevine downy mildew, *Plasmopara viticola*, comparative genomics

INTRODUCTION

The use of marker-assisted selection (MAS) has expedited the improvement of economically important traits in grapevines (*Vitis* sp.) since its incorporation in breeding programs. Starting with restriction fragment length polymorphisms (RFLPs) used to distinguish individuals (Striem *et al.,* 1990), the technology has grown to allow for the high-throughput screening of an ever-growing list of available loci using rhAmpSeq local haplotype markers, based on highly-multiplexed, amplicon markers targeting the *Vitis* core genome (Zou *et al.,* 2020). Microsatellite markers such as simple sequence repeats (SSRs) have long been a widely adopted and highly useful step in this progression as they are multi-allelic by design and complement the high heterozygosity intrinsic to *Vitis* (Arnold *et al.,* 2002). Not without their disadvantages, the broad use of SSRs in genetic mapping studies created opportunities for the comparison of alleles across breeding and mapping populations (Fischer *et al.,* 2004). This was crucial for the identification and validation of loci influencing important phenotypes, including resistance to destructive plant diseases such as grapevine downy mildew.

Grapevine downy mildew, caused by the oomycete *Plasmopara viticola,* is among the most economically damaging diseases in vineyards in humid climates, such as the eastern United States and much of Europe (Koledenkova *et al.,* 2022). Once grapevine downy mildew takes hold, potentially infecting all green tissues, producers often rely on extensive chemical applications for control. As this increases the risk of the pathogen developing fungicide resistance (Massi *et al.,* 2021), many breeders have focused substantial efforts toward selecting genetic resistance within their released cultivars. This has led to the identification of over 35 Rpv (resistance to *P. viticola*) loci, each conferring resistance of varying strengths (*Vitis* International Variety Catalogue: www.vivc.de). Since *V. vinifera*, the most commonly cultivated species in wine and table grape production, is predominately susceptible (Cadle-Davidson, 2008), resistance is often introgressed from the North American and Asian *Euvitis* subgenus (Di Gaspero *et al.,* 2012; Peng *et al.,* 2024). One of the most selected resistance loci, *Rpv3*, resides on the lower arm of chromosome 18 and enacts a race-specific hypersensitive response when triggered by *P. viticola* (Casagrande *et al.,* 2011).

The *Rpv3* QTL was originally identified through the combined works of Fischer *et al*. (2004) and Welter *et al*. (2007) in the wine grape 'Regent' and later tied to the resistance in the hybrid 'Bianca' (Bellin *et al.,* 2009). Di Gaspero *et al*. (2012) later performed an extensive survey of 580 grapevines and identified seven conserved haplotypes based on the locus flanking SSR markers UDV305 and UDV737. The most common haplotype found was *Rpv3*$^{299\text{-}279}$, now designated as *Rpv3.1,* was connected to the resistance found in both 'Regent' and 'Bianca'. The second most conserved haplotype through 'Munson' ('Jaeger 70'), *Rpv3*$^{\text{null-}297}$, is now known as *Rpv3.2* after it was confirmed to confer downy mildew resistance through QTL mapping (Zyprian *et al.,* 2016). The final conversed haplotype to receive an allelic designation, *Rpv3*$^{\text{null-}271}$, was named *Rpv3.3* and descended from 'Noah' into the complex hybrid 'Merzling' (Vezzulli *et al.,* 2019). Candidate genes for *Rpv3*, TNL-NBS-LRR (*TNL*) gene paralogs and a leucine-rich repeat kinase (*LRRk)*, have been identified through controlled inoculation and gene expression analysis within individuals carrying *Rpv3.1* (Foria *et al.,* 2020; Wairich *et al.,* 2022). Separately, a resistance locus identified in the *V. aestivalis*-derived 'Norton', *Rpv27*, co-locates with *Rpv3* (Hammers *et al.,* 2017; Sapkota *et al.,* 2019) but is distinguished from *Rpv3* through its haplotype's absence from the conserved list in Di Gaspero et al (2012).

While *Rpv3.1* is often found to confer the strongest level of resistance, followed by *Rpv3.2* and then *Rpv3.3*, there is growing evidence for race-specificity on grapevines carrying *Rpv3* alleles (Cadle-Davidson, 2008; Delmotte *et al.,* 2014; Heyman *et al.,* 2021; Paineau *et al.,* 2022). The issue of race-specificity at this locus is further complicated by the fact that the allele designations are intrinsically tied to SSR markers with limited resolution. As pathogens evolve to overcome these resistance genes, SSR markers cannot be relied upon to capture sequence variation within individuals carrying the same *Rpv3* allele, hampering the ability to track the co-evolution of pathogens and resistance genes at this locus. The potential discrepancies this introduces coupled with the technological advances in genomic sequencing and bioinformatics present the means and opportunity to improve upon the limited resolution of *Rpv3* and *Rpv27* currently provided by screening with SSR markers. Using the SSR-based allelic designations from Di Gaspero *et al*. (2012) (*Rpv3*) and Sapkota *et al*. (2019) (*Rpv27*), the PacBio long-read (Hon *et al.,* 2020) genome assemblies of eight grapevines were used to compare the structural and candidate gene copy number variation among and between haplotype alleles. In doing so, the creation of more informative, higher resolution markers for MAS can be designed and utilized by breeders in selecting for improved resistance to grapevine downy mildew.

MATERIALS AND METHODS

1. Genome Assemblies

The genome assemblies of eight grapevines, 'Catawba', 'Concord', 'Chambourcin', 'Horizon', MN1264, 'Norton', NY84.0101.03 and PN40024, were used in this study. These individuals were included because they were known or implicated via SSRs as carriers for either specific *Rpv3* alleles or *Rpv27*. Among the French-American hybrids, NY84.0101.03 is heterozygous for *Rpv3.1,* 'Horizon' and MN1264 both carry single copies of *Rpv3.2,* while 'Chambourcin' is heterozygous for both *Rpv3.1* and *Rpv3.2* (Di Gaspero *et al.,* 2012; Clark *et al.,* 2018; Patel *et al.,* 2023; Reisch, 2024). 'Norton' is commonly described as being derived from *V. aestivalis* and is one of the known carriers of *Rpv27* (Hammers *et al.,* 2017; Sapkota *et al.,* 2019). 'Catawba' and 'Concord' are related hybrids between *Vitis labrusca* and *V. vinifera* that date back to the early to mid-1800s. Specifically, 'Catawba' is an F_1 of *V. labrusca* and *V. vinifera* 'Semillon', while 'Concord' is the product of a 'Catawba' backcross to *V. labrusca* (*Vitis* International Variety Catalogue: www.vivc.de). While both were found to carry the SSR fragment lengths for *Rpv3.3*,

neither could be tied to a known source through pedigree. Lastly, PN40024 is a highly homozygous *V. vinifera,* recently shown to originate from the repeated selfing of 'Helfensteiner', an F_1 of 'Pinot noir' (Velt *et al.,* 2023) and is often used as the primary reference genome for grapevines.

Through the use of haplotype-resolved genome assemblies, the *Rpv3* / *Rpv27* region of sixteen haploid genome assemblies were characterized. Genome assemblies for 'Catawba', 'Concord', MN1264, 'Norton', and NY84.0101.03 were constructed at Cornell University while 'Horizon' was assembled at the University of California–Davis. Genome assembly followed the same methodology described in detail by Zou et al. (2023) for the *Vitis* x *doaniana* 'PI 588149' genome assembly. Briefly, SMRTbell Template Prep Kit SP v2 (PacBio, CA, USA) libraries were constructed from high molecular weight DNA that was filtered for DNA between 15–20 kbp using BluePippin (Sage Science, MA, USA). The libraries were then sequenced with a PacBio Sequel II using 1 SMRT cell by the DNA Sequencing and Genotyping Center at the University of Delaware. The resulting PacBio reads were then used to construct two phased assemblies using Hifiasm (v0.16.0) (Cheng *et al.,* 2021). 'Chambourcin' and PN40024 had preexisting, publicly available genome assemblies that were used in this study. The 'Chambourcin' assembly constructed by Patel *et al*. (2023) was diploid with haplotypes separated into 'primary' and 'haplotig' assemblies and was accessed via the article's supplemental data. PN40024, as an inbred accession, was constructed as a haploid genome assembly in its role as reference genome. However, including both high quality versions of PN40024, PN40024.v4 (Velt *et al.,* 2023) and PN_T2T (Shi *et al.,* 2023), allowed for a bioinformatic comparison of these versions in addition to the opportunity to update the physical positions of *Rpv3* and *Rpv27* in the latest versions of the reference genome. Both versions of PN40024 were downloaded from grapedia.org/genomes.

2. Characterizing the *Rpv3* and *Rpv27* Loci

As SSR markers are intrinsically tied to the allele classification and demarcation of *Rpv3* and *Rpv27*, the primer sequences of associated SSR were used to validate the presence and the physical boundaries of these loci within each diploid assembly (Table 1).

SSR*	Forward Primer	Reverse Primer
VVCS1	GGAAGACATCATACTTCCAT	CTTGTTCATTCTTCGAAAGG
UDV305	TGGTGCAATGGTCATAATTT	GAGGAAAAGAGAAAGCAAAGA
UDV730	CAGCAACTACCACTGGCTCA	CAACTGAGGAAGAGCCCAAA
UDV734	TGTGTAATGCAAGGCCAACT	AAGACGTTCAATACCCACATGA
UDV736	GGATTCAGAACCACCGTTGA	GAGCAATCGAGGCAGAAAAT
UDV737	TTTGCATGCGATACCTGAAG	TCCTGCAGCTGTTGACGATA

TABLE 1. SSR primer sequences associated with *Rpv3* and *Rpv27*.

*Abbreviations: VVCS1, VVCS1H077H16R1-1.

Using BBMap (v39.03) (Bushnell, 2024) under default parameters, both forward and reverse primer sequences from six SSR markers were aligned to all sixteen haplotypes from eight assemblies, separately. Based on the predicted fragment lengths from BBMap, each haplotype assembly was then assigned to an *Rpv3* allele or *Rpv27* based on the combination of UDV305–UDV737 or VVCS1H077H16R1-1–UDV737 for *Rpv3* (Di Gaspero *et al.,* 2012) or *Rpv27* (Sapkota *et al.,* 2019), respectively. Fragment length combinations for *Rpv3* allele assignment, as UDV305–UDV737, were: *Rpv3.1,* 299–279; *Rpv3.2*, null–297; and *Rpv3.3*, null–271 while the fragment length for *Rpv27,* as VVCS1H077H16R1-1–UDV737, was 99—294. An exact match was not required, however, given that small differences were expected between the *in-silico* fragment lengths derived through BBMap and the reported PCR amplification products for each allele. Three additional SSRs, UDV730, UDV734, and UDV736, were included as associated markers that span the gap between the diagnostic pairs described above.

In order to focus solely on *Rpv3* and *Rpv27,* the physical positions of SSR markers VVCS1H077H16R1-1 and UDV737, the most physically distant pair, were used to isolate the region from the rest of each haplotype assembly using the 'seqinr' package (Charif & Lobry, 2007) to manually isolate the sequence in R (R Core Team, 2023). In most of the haplotype assemblies, the *Rpv3* / *Rpv27* region was contiguous. Extensions of 5 kb and 100 kb were added to the positions of VVCS1H077H16R1-1 and UDV737, respectively. A larger extension was included beyond UDV737 to include more of the neighboring NLR (Nucleotide-binding Leucine-rich Repeat) gene cluster found to reside nearby. For haplotype assemblies where the SSRs were split across multiple contigs, all-to-all genome alignments were performed using 'nucmer' with default parameters from MUMmer4 (v4.0.0) (Marçais *et al.,* 2018). The discontiguous haplotype was aligned to a contiguous haplotype with the same allele. This allowed for the visual selection of contigs via 'mummerplot' and the formation of an *Rpv3* / *Rpv27* region for each haplotype assembly. Once the haplotype assemblies were narrowed down, AUGUSTUS (v3.4.0) (Stanke *et al.,* 2008) was used for gene prediction, followed by functional annotation with diamond (v2.1.8) (Buchfink *et al.,* 2021) and Blast2GO (v1.5.1) (Gotz *et al.,* 2008) each under default parameters. NLR genes were annotated using NLR-Annotator (Steuernagel *et al.,* 2020)

with their functionality and completeness predicted using NLRexpress (Martin *et al.,* 2022), again under default parameters. Visualization of the *Rpv3* / *Rpv27* regions, including positions of mapped SSR and annotated NLR genes was produced in Python (v3.9) using custom script incorporating tools from 'pyGenomeViz' (v0.4.4) (Moshi, 2024).

3. Candidate Gene Analysis

The candidate genes conferring *Rpv3.1* downy mildew resistance were first identified by Foria *et al*. (2020) and later corroborated and expanded upon by Wairich et al (2022). These candidate genes were two TIR-NBS-LRR (*TNL*), 'VIT_18s0041g01330' (*TNL1*) and 'VIT_18s0041g01340' (*TNL2*), and a leucine-rich repeat kinase (*LRRk*), 'VIT18s0041g01350'. Both articles demonstrated the role *TNL2* (as paralogs *TNL2a* and *TNL2b* in *Rpv3.1)* played in triggering a defense response through expression analysis. Only Wairich *et al*. (2022), however, found evidence that *TNL1* and *LRRk* may also play a role. All three gene models were included here for completeness in characterizing the locus. The reported gene model identifiers were based on a previous version of the PN40024 reference genome, however. In order to characterize the presence, functionality, and abundance of these genes, the gene model identifiers were updated to their PN40024.v4 counterparts through the PN40024 reference genome browser provided by grapegenomics.com (hosted by UC-Davis). These translations were: *TNL1*, 'Vitvi18g02077'; *TNL2*, 'Vitvi18g03133'; and *LRRk*, 'Vitvi18g02080'. The genomic sequences for these three genes were aligned to each haplotype assembly using nucleotide BLAST (Camacho *et al.,* 2009), (-max_target_seq 5 -evalue 1e-10) including the diploid *Muscadinia rotundifolia* 'Trayshed' assembly (Minio *et al.,* 2022) as an outgroup. The high sequence similarity between *TNL1* and *TNL2* made it necessary to identify short, 60 bp sequences of high divergence that could be used to sort through the blast results. These sequences were identified using a combination of R (R Core Team, 2023) and alignment in MEGA11 (Tamura *et al.,* 2021). These short sequences were then blasted back to the extracted alignment results of the initial

Grapevine	Assembly Source	Haplotype	N50 (Mb)	Complete BUSCO (%)	SSR Allele (UDV305-UDV737)
Catawba	Cornell University	Hap1	14.0	98.3	*Rpv3.3** (null-271)
		Hap2	13.6	96.1	*V. vinifera* (null-287)
Chambourcin	Patel *et al.* (2023)	Primary	23.3	97.9	*Rpv3.1* (299-279)
		Haplotig	-	-	*Rpv3.2* (null-297)
Concord	Cornell University	Hap1	21.0	97.7	*V. vinifera* (null-287)
		Hap2	20.4	97.5	*Rpv3.3** (null-271)
Horizon	UC-Davis	Primary	14.9	98.7	*Rpv3.2* (null-297)
		Haplotig	-	-	*Rpv3.3** (null-271)
MN1264	Cornell University	Hap1	9.4	97.3	*Rpv3.2* (null-297)
		Hap2	7.8	97.1	NC (323-279)
Norton	Cornell University	Hap1	19.8	98.0	NC (null-291)
		Hap2	17.4	98.3	*Rpv27#* (100-290)
NY84.0101.03	Cornell University	Hap1	4.9	95.8	*Rpv3.1* (299-279)
		Hap2	5.6	95.8	NC (321-312)
PN40024	Velt *et al.* (2023)	PN40024.v4	26.9	98.1	*V. vinifera* (null-287)
	Shi *et al.* (2023)	PN_T2T	25.9	98.5	*V. vinifera* (null-287)

TABLE 2. Genome assembly statistics and *Rpv3/Rpv27* allele.

*SSR alleles designated as *Rpv3.3* were based solely on SSR fragment lengths and were unable to be confirmed via pedigree analysis. #*Rpv27* fragment lengths (VVCS1H077H16R1-1–UDV737); SSR alleles labeled *V. vinifera* refer to haplotypes descending from *V. vinifera*, while NC reflects non-characterized haplotypes. Contig N50 and BUSCO scores were skipped for haplotig assemblies as they do not represent the complete genome.

blastn (-evalue 1e-10). Manual classification of the results to either *TNL1* or *TNL2* was based, in part, on the presence and quality of the alignment of these short sequences. Alignment quality was assessed based on the combination of percent identity and alignment length. Multiple sequence alignment of the resulting *TNL1, TNL2,* and *LRRk* sequences from each haplotype genome was followed by the construction of neighbor-joining trees using MEGA11 and visualized in iTOL (v5) (Letunic & Bork, 2021). In order to compare the sequence similarity among the *LRRk* from each haplotype, pairwise distances were calculated under default settings in MEGA11.

RESULTS

1. Genome Assemblies

In order to have high quality representation of each haplotype allele at *Rpv3* and *Rpv27*, assemblies of six new grapevines were constructed. These grapevines, 'Catawba', 'Concord', 'Horizon', MN1264, 'Norton', and NY84.0101.03 were included alongside 'Chambourcin' and PN40024 to account for alleles *Rpv3.1*, *Rpv3.2*, *Rpv3.3*, and the co-located *Rpv27* as assigned based on diagnostic SSR. The primary or haplotype-resolved contigs for the six new diploid assemblies ranged in contig N50 from 4.9–21 Mb with complete BUSCO scores from 95.8–98.7% (Table 2).

The combination of SSR markers UDV305 and UDV737, or VVCS1H077H16R1-1 and UDV737 for *Rpv27,* were used to classify each haploid assembly with an *Rpv3* allele according to the fragment lengths described in Di Gaspero *et al*. (2012). There were two assembled haplotypes of *Rpv3.1,* Chambourcin Primary and NY84.0101.03 Hap1. *Rpv3.2* was assembled three times from Chambourcin Haplotig, Horizon Primary, and MN1264 Hap1. Potential haplotypes of *Rpv3.3* based on SSRs were assembled from Catawba Hap1, Concord Hap2, and Horizon Haplotig. Norton Hap 2 was the only instance of *Rpv27*. An additional conserved haplotype from Di Gaspero *et al*. (2012) representing a *V. vinifera* background, UDV305: null–UDV737: 287, from PN40024.v4, PN_T2T, Concord Hap1, and Catawba Hap2. The final three haplotypes, MN1264 Hap2, Norton Hap1, and NY84.0101.03 Hap2 were distinct from each other and have yet to be characterized.

2. Characterizing the *Rpv3* and *Rpv27* Loci

Using the alignment positions of the six SSR markers, the *Rpv3* / *Rpv27* region was extracted from each haplotype assembly based on the two most physically separated markers, VVCS1H077H16R1-1 and UDV737. Across all haplotypes, this region ranged from 0.8 to 1.7 Mb (Table S1). Both examples of *Rpv3.1* were contiguous in their assemblies and covered a physical distance of 1.36 Mb and 1.40 Mb on the Chambourcin Primary and NY84.0101.03 Hap1 assemblies, respectively. For *Rpv3.2*, both the Chambourcin Haplotig and MN1264 Hap1 assemblies were contiguous and spanned 1.3 Mb, while the Horizon Primary *Rpv3.2* was not contiguous. This assembly was thusly aligned to Chambourcin Haplotig, another *Rpv3.2*, contig 'vitin_chambo_h_18_02'. The *Rpv3.2* from Horizon Primary was scaffolded using two contigs ('VITHorizon_Primary000139F' and 'VITHorizon_Primary000043F') spaced roughly 3 kb apart for a total length of 1.19 Mb (Figure S1). More variation in length existed among the three representatives of *Rpv3.3*. Catawba Hap1 and Concord Hap2 were both contiguous and 1.29 and 1.34 Mb in length. The third, Horizon Haplotig, was not contiguous and also lacked successful alignments for both VVCS1H077H16R1-1 and UDV730. Regardless, the Horizon Haplotig assembly was aligned to the Concord Hap 2 contig 'h2tg000005l' and scaffolded using four contigs with cumulative added spacing of 125 kb for a total length of 0.8 Mb (Figure S2). The single carrier of *Rpv27*, Norton Hap2, had a contiguous length of 1.3 Mb. The *V. vinifera* haplotype alleles were all contiguous and consistent in length, with the two versions of PN40024 at 1.52 Mb and both Concord Hap1 and Catawba Hap2 at 1.53 Mb. Of the remaining three haplotype assemblies, NY84.0101.03 Hap2 and Norton Hap1 were both contiguous yet varied in length at 1.43 Mb and 1.7 Mb, respectively. Lastly, the MN1264 Hap2 haplotype was not contiguous and due to its novelty within the study was aligned to the PN_T2T assembly contig 'PN18', resulting in a scaffolded region of 1.27 Mb consisting of two contigs, spaced 12.6 kb apart (Figure S3). The extracted genomic sequences for *Rpv3*/*Rpv27* haplotypes, including those scaffolded for this analysis, are provided in Additional Data 1.

Visualization of the extracted *Rpv3*/*Rpv27* regions of each haplotype, specifically the distribution of the SSR markers and predicted gene structure, allowed for the resolution of existing sequence variation within and among haplotype alleles. While the gene structure between individuals carrying the same *Rpv3* allele differed, all haplotypes became more consistent as they approached UDV737, especially within allelic groups (Figure 1).

For *Rpv3.1*, the two haplotype assemblies showed strong similarities throughout the 157 and 159 predicted gene features in Chambourcin Primary and NY84.0101.03 Hap1 and are nearly identical between UDV736 and UDV737. For *Rpv3.2*, Chambourcin Haplotig and MN1264 Hap1 shared more structural similarity than with Horizon Primary. This was also reflected in their gene feature predictions, both containing 136 features compared to 121 for Horizon Primary. Lastly, *Rpv3.3* was the least consistent, with each haplotype showing a unique distribution of their SSR and predicted gene structure. Concord Hap 2 had the most gene features with 145, then Catawba Hap1 with 132, followed by Horizon Haplotig at 63 features. *Rpv27* maintained similar gene structure to the *Rpv3* alleles nearer to UDV737 and included 145 gene feature predictions. The four *V. vinifera* haplotypes had reasonably similar structure and ranged between 167 and 173 predicted gene annotations. The remaining three haplotypes had 144 predicted gene features for NY84.0101.03 Hap2, 216 for Norton Hap 1, and 133 for MN1264 Hap2. An annotation file containing the regional

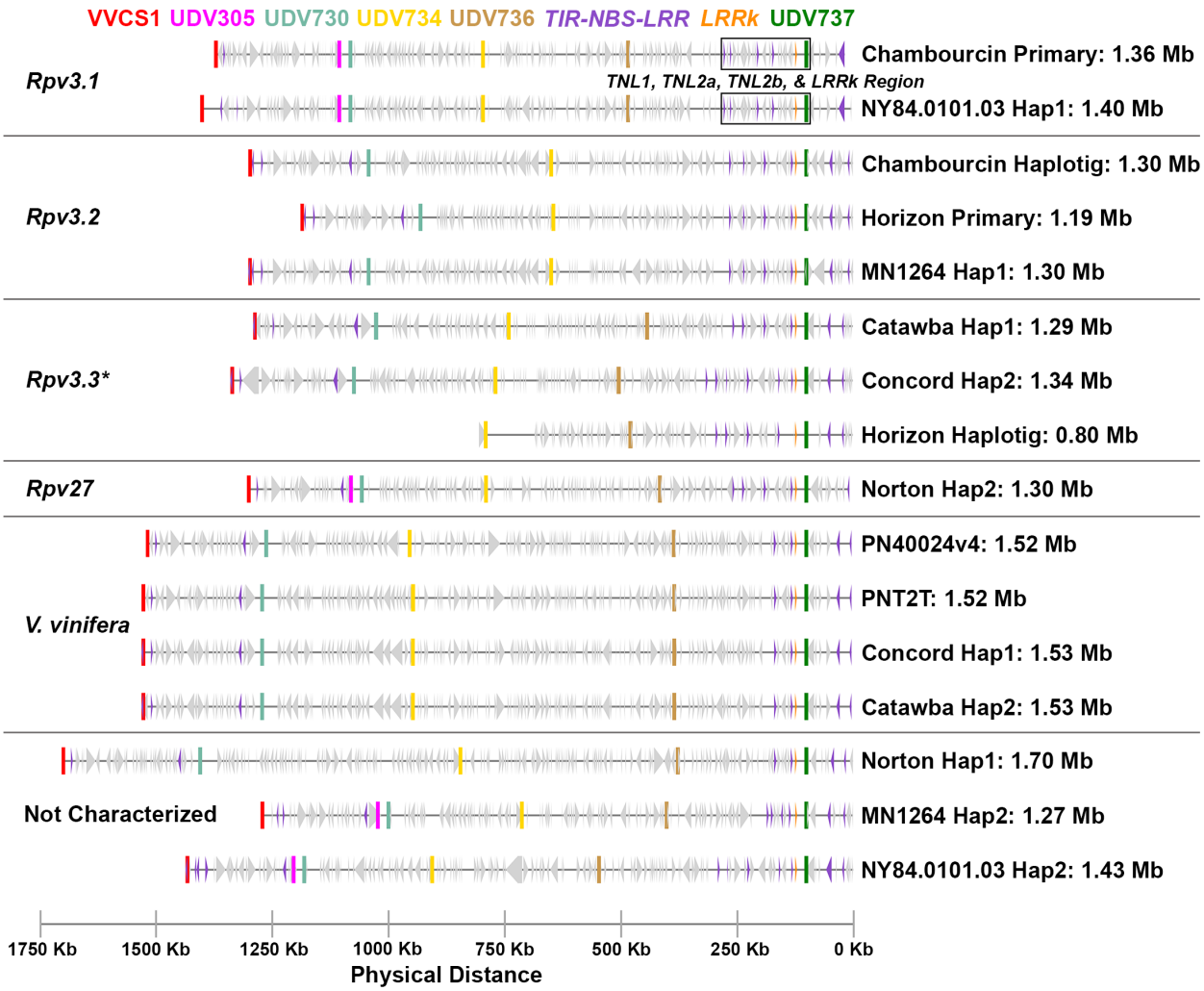


FIGURE 1. *Rpv3* and *Rpv27* region SSR alignments and annotated genes by SSR haplotype.

▫ VVCS1: VVCS1H077H16R1-1; *Haplotypes labeled as *Rpv3.3* were based solely on SSR fragment lengths and were unable to be confirmed via pedigree analysis. The black boxes on Chambourcin Primary and NY84.0101.03 Hap1 show the within-haplotype *Rpv3.1* candidate gene region containing *TNL1*, *TNL2a*, *TNL2b*, and *LRRk*. Gray arrows within each haplotype are predicted gene feature annotations. The regional alignments are anchored to the position of SSR marker UDV737 (green) to facilitate comparison among haplotype alleles.

SSR positions and predicted gene annotations is provided in Additional Data 2.

3. Candidate Gene Analysis

Three candidate genes have been found in connection to the resistance conferred by *Rpv3.1*. The first *TNL*, *TNL2* was identified by Foria *et al*. (2020) as a pair of paralogs, *TNL2a* and *TNL2b* with the second *TNL*, *TNL1,* and a nearby *LRRk* added later by Wairich *et al*. (2022). The gene model identifiers were translated to the PN40024.v4 reference genome (Velt *et al.,* 2023), functionally annotated, and aligned to the extracted *Rpv3*/*Rpv27* regions. In every analyzed haplotype, the candidate genes clustered closely to UDV737, within 220 kb, with a single copy of the *LRRk* roughly 25 kb upstream (Figure 2).

Pairwise comparisons of the *LRRk* from each haplotype revealed high amino acid sequence similarity, with a maximum divergence of just above 4 % (Table S2). The number, functionality, and position of the *TNL* genes relative to UDV737 were more varied across alleles compared to the *LRRk*. Consistent in both *Rpv3.1*, there was one complete copy of *TNL1* roughly 178 kb away from UDV737, followed by a partial *TN* and two complete copies of *TNL2* which correspond directly to the *TNL2a* and *TNL2b* described in Foria et al. (2020). *Rpv3.2* was similar with *Rpv3.1* in terms of gene frequency and functionality, however their organization differed. In all three examples of *Rpv3.2,* there were two complete *TNL2* copies flanking a *TNL1* homolog and a *TNL1* predicted pseudogene, with the furthest *TNL2* alignment roughly 166 kb upstream of UDV737. All three SSR-based haplotypes of *Rpv3.3* differed in gene distribution and length. Catawba Hap1 and Horizon Haplotig both had two complete copies of *TNL1,* one complete copy of *TNL2*, and one *TNL2* pseudogene. The *Rpv3.3* allele from Concord Hap2 had the greatest number of *TNL* alignments, consisting of three complete *TNL1*, one complete *TNL2*, and two *TNL2*

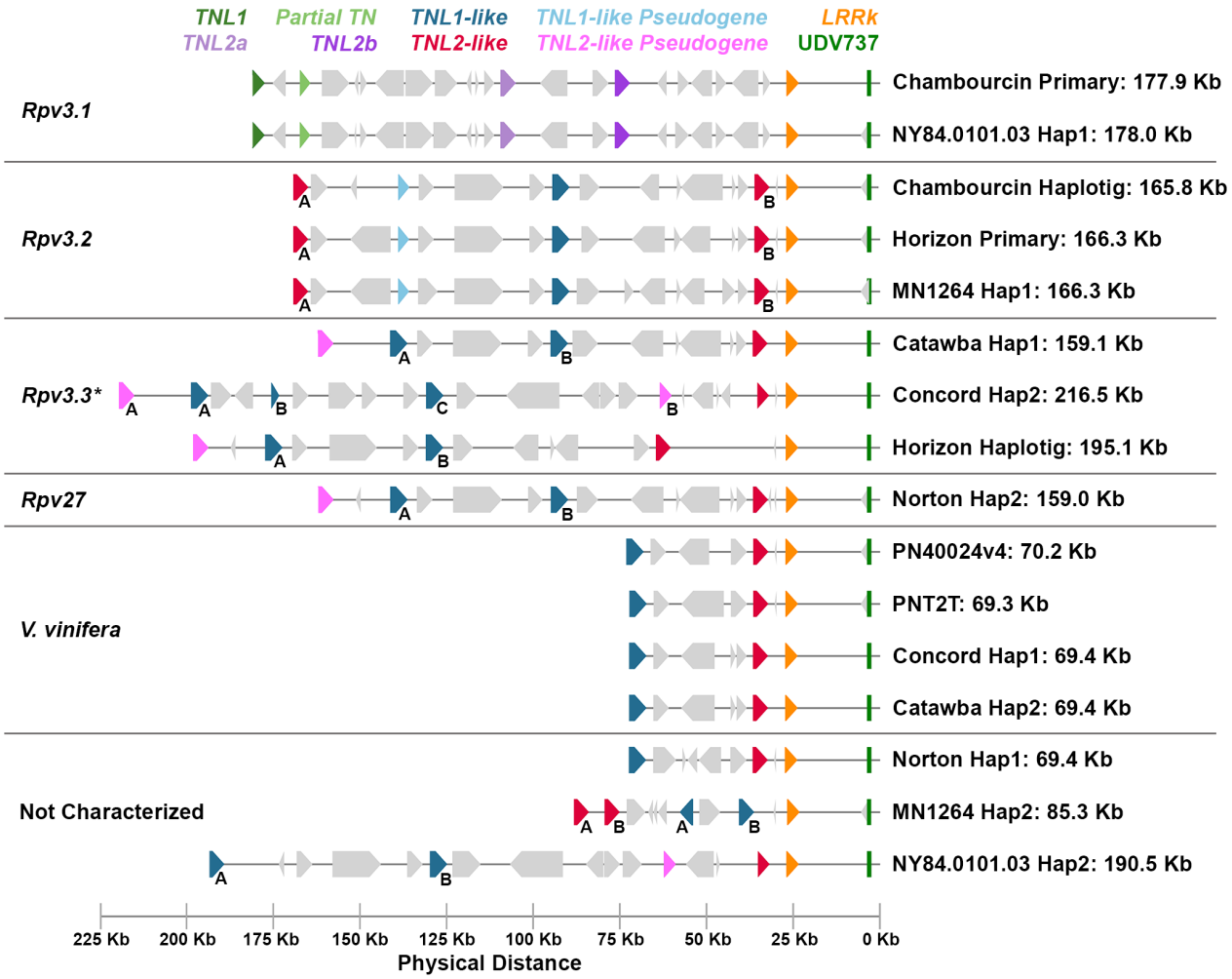


FIGURE 2. *Rpv3.1* candidate gene positions and predicted functionality by haplotype allele.

▫ *Haplotypes labeled as *Rpv3.3* were based solely on SSR fragment lengths and were unable to be confirmed via pedigree analysis. Gray arrows within each haplotype are predicted, non-candidate gene feature annotations. The letters next to some genes serve to distinguish multiple genes of the same type for comparisons between Figure 2 and Figure 3. The distinction between complete, partial, and pseudogene was based on in-silico prediction using NLRexpress. Each region is anchored to the position of SSR marker UDV737 (green bar) to allow for comparison among haplotype alleles.

pseudogenes. In all three *Rpv3.3,* a *TNL2* pseudogene was the furthest from UDV737 at 159.1 kb, 195.1 kb, and 216.5 kb for Catawba Hap1, Horizon Haplotig, and Concord Hap2, respectively. Norton Hap2's *Rpv27* was most similar in *TNL* gene copies and functionality to the *Rpv3.3* alleles from Catawba Hap1 and Horizon Haplotig. The four *V. vinifera* haplotypes and Norton Hap1 all had complete single copies of each *TNL* and were within 69.3–70.2 kb of UDV737. The final two haplotypes differed. MN1264 Hap2 had two complete copies each of *TNL1* and *TNL2* within 85.3 kb while NY84.0101.03 Hap2 had one complete copy of *TNL2*, one *TNL2* pseudogene, and two copies of *TNL1* within 190.5 kb of UDV737.

The sequences of the *TNL1*, *TNL2*, and *LRRk* gene copies from each haplotype were extracted from their assemblies, aligned, and used to produce neighbor-joining trees. The alignment results from both haplotypes of *Muscadinia rotundifolia* 'Trayshed' were also included to serve as outgroups. The *TNL1* and *TNL2* gene copies separated predictably when combined into an unrooted tree (Figure S4), and the *Rpv3* alleles largely grouped together among the *LRRk* from each haplotype (Figure S5). The multiples of each *TNL* gene copy from *Rpv3.1* and *Rpv3.2* grouped together while *Rpv3.3* was less consistent and grouped closely with *Rpv27* (Figure 3A to 3B).

Among the *TNL1* copies from each haplotype, the *TNL1* from *Rpv3.1* grouped most closely with the complete *TNL1-like* alignments from *Rpv3.2* and those from *Rpv3.3* and *Rpv27* closest to UDV737 (Figure 3A). The partial *TN* from *Rpv3.1* was also predictably more similar to *TNL1* than *TNL2* and grouped closely with the original *TNL1*. The haplotype from Norton Hap1 was more similar to the *V. vinifera* haplotypes than any other for both *TNL1* and *TNL2*. While the *TNL1-like* pseudogene from *Rpv3.2* grouped closely with the complete *TNL1-like* A's from both *Rpv3.3* and *Rpv27*, the inverse was true for *TNL2* (Figure 3B). The *TNL2-like* pseudogenes from

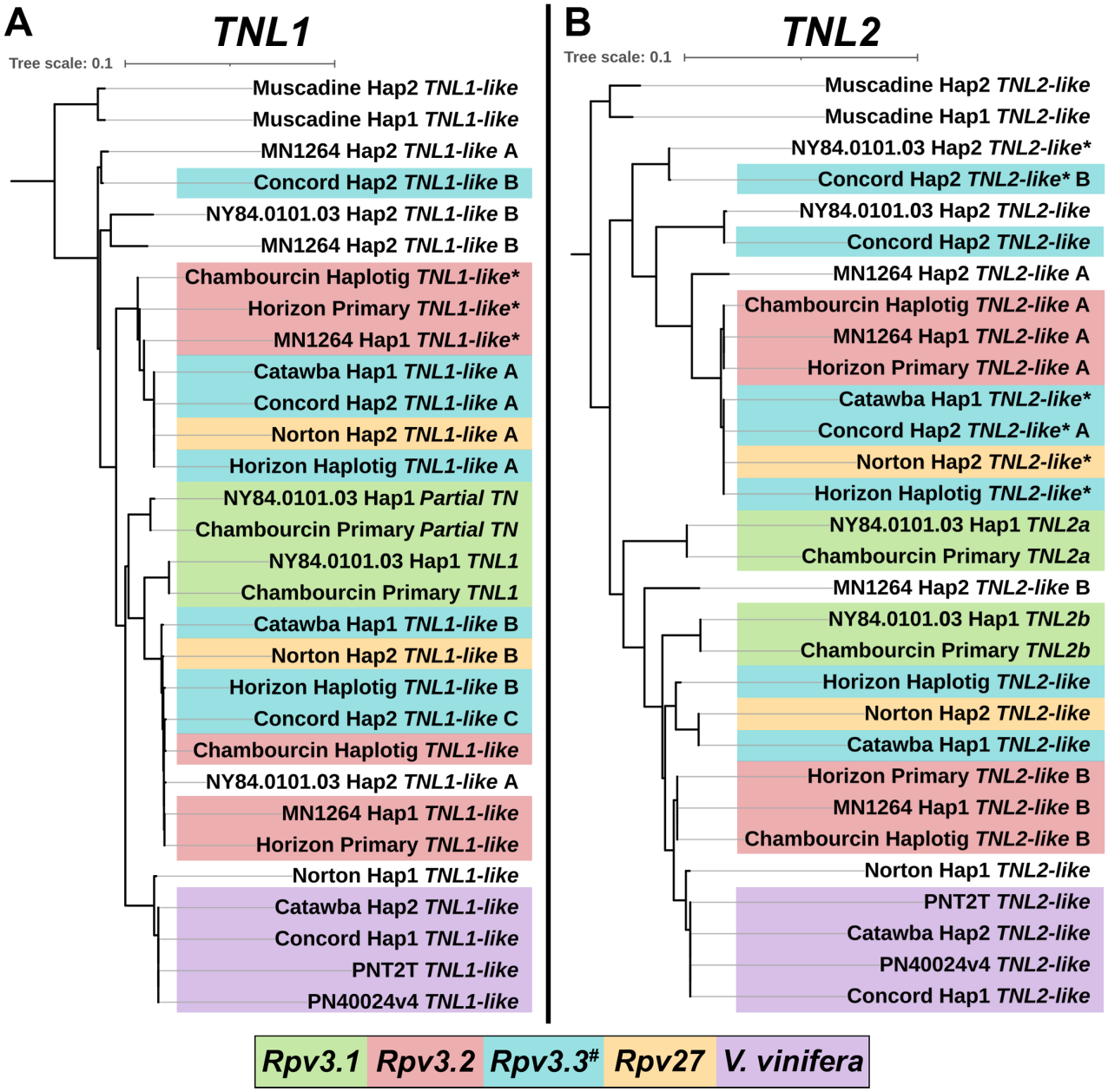


FIGURE 3. Rooted neighbor-joining trees of *TNL1* (A) and *TNL2* (B) gene copies across all haplotypes.

[a] #Haplotypes labeled as *Rpv3.3* were based solely on SSR fragment lengths and were unable to be confirmed via pedigree analysis. In both panels, the background color indicates the haplotype's SSR–determined *Rpv3/Rpv27* allele as *Rpv3.1*: green, *Rpv3.2*: red, *Rpv3.3*: blue, *Rpv27*: orange, or *V. vinifera*: purple. Haplotypes without a background color represent those from the outgroup, Muscadine, or are non-characterized haplotypes as listed in Table 2. Labels with an asterisks (*) were predicted pseudogenes, while those followed by letters correspond to genes labeled with letters in Figure 2, allowing for direct comparison between figures.

Rpv3.3 and *Rpv27* were more similar to the *TNL2-like* A's from *Rpv3.2*. Both paralogs of *TNL2* in *Rpv3.1*, *TNL2a* and *TNL2b* were more closely grouped than the pair of *TNL2-like* alignments from *Rpv3.2*.

DISCUSSION

Using the phased genome assemblies of eight diploid grapevines, the *Rpv3* and co-locating *Rpv27* loci were characterized to compare the structural variation within and among haplotypes. In doing so, this work showed that variation exists within individuals carrying the same *Rpv3* allele, especially in *Rpv3.2* and *Rpv3.3,* and demonstrates that the widely used diagnostic SSR markers lack the resolution necessary to capture variation at the locus. In comparing the copy number and structural variation of the *Rpv3.1* candidate genes in each haplotype, the close relationship between the genes in *Rpv3.3* and *Rpv27* suggest the need for additional candidate gene analyses to validate the genetic mechanisms underlying their resistance. This work represents an important step in designing high density markers for improved coverage of this multiallelic resistance locus.

The concept of *Rpv3* haplotypes introduced by Di Gaspero *et al*. (2012) provided pioneering insight into the challenges faced when characterizing resistance loci. While most haplotypes at a resistance locus confer susceptibility, grape scientists are now demonstrating functional allelic variation among resistant haplotypes that translates into quantitative and/or mechanistic differences in resistance phenotypes. This concept is even more impressive considering it was built upon a low-resolution marker platform, namely two SSRs spaced, at most, 1.7 Mb apart as shown in the current study. In quantitative phenotypic differences among *Rpv3* haplotypes, *Rpv3.*1 typically offers the greatest resistance to grapevine downy mildew and therefore is the most selected allele (Di Gaspero *et al.,* 2012; Foria *et al.,* 2020). The resistances conveyed by *Rpv3.2* and *Rpv3.3* tend to be weaker (Foria *et al.,* 2018), less reproducibly detected, and sometimes eliminated from breeding programs in favor of stronger alternative loci. Although *Rpv27* may confer the strongest resistance among these haplotypes by effect size (Sapkota *et al.,* 2019), it has not been as widely characterized.

We explored *Rpv3* haplotypes more deeply to determine the level of variation within and among haplotypes both in structure and candidate gene sequence. For the genomes analyzed here, most of the alleles defined by Di Gaspero *et al*. (2012) are structurally conserved (at least moderately) across the SSR haplotype, and particularly in the 220 kb candidate gene region upstream of UDV737. The exception was *Rpv3.3*, which showed significant structural variation among individuals positive for this allele based on SSR haplotypes. While the *Rpv3.1* and *Rpv3.2* haplotypes were supported by pedigree connections to known sources, this cannot be said for 'Catawba', 'Concord', or 'Horizon' to *Rpv3.3*. While the potential for these connections is dependent on the accuracy of reported pedigrees, another potential explanation could be size homoplasy between haplotypes connected to *V. labrusca* and 'Merzling', where *Rpv3.3* was first described. Size homoplasy of SSRs is the occurrence of amplification products of identical size in unrelated individuals which has been described in microsatellite markers and can result from mutations and recombination events within SSR flanking sequences (Grimaldi & Crouau-Roy, 1997). It has been documented but not well studied in grapevines (Battilana *et al.,* 2013).

One hypothesis underlying this study was that the phenotypic variation observed among resistant haplotypes might be explained by the presence or sequence of their candidate genes. This hypothesis was supported by *Rpv3.1,* with divergent sequences relative to other resistant and susceptible alleles for *TNL1*, *TNL2a*, and *TNL2b* as shown by the neighbor-joining trees. Although the true inclusion of *Rpv3.3* in this work is questionable, their candidate gene sequences clustering closely with those from *Rpv3.2* may be reflected in the minor phenotypic differences between alleles. What was most surprising was that all *Rpv27 TNL*s clustered tightly with *Rpv3.3*, suggesting one possibility that the genetic basis of *Rpv27* resistance may lie outside this *TNL* region given the stronger resistance conferred by *Rpv27* compared to *Rpv3.3*. Another alternative still could be that the included *Rpv3.3* SSR haplotypes bear more genetic similarity to *Rpv27* irrespective of the SSR haplotype. As to how these observations can be tied to phenotypic variation seen among *Rpv3* alleles requires further research.

Of the resistance alleles characterized, *Rpv3.1* is the only one to have candidate genes validated through expression analysis and functional research (Foria *et al.,* 2020; Wairich *et al.,* 2022). Their presence in every haplotype and *M. rotundifolia* indicates that they are highly conserved, yet have been subjected to evolutionary events that resulted in their divergence into independent alleles. Foria *et al*. (2020) suggested an evolutionary model from a common ancestral haplotype leading to the PN40024 and *Rpv3.1* haplotypes involving tandem segmental duplication and the movement of retrotransposons. Where the other haplotypes fit into their evolutionary timeline remains unclear along with the scope of influence these candidate genes have beyond *Rpv3.1*.

In making selections for improved grapevine downy mildew (*P. viticola*) resistance, plant breeders can rely on MAS to stack multiple resistance genes and expedite the release of new varieties and cultivars. While an individual SSR may typically have tens of alleles, they are based on sizes that can be attained convergently and may not capture informative underlying sequence variation. Across the *Rpv3* haplotype defined by SSRs, selection appears more targeted toward one side of the locus, near the *Rpv3.1* candidate genes and UDV737. This would suggest breeders have focused higher selection pressure on this roughly 160–220 kb region rather than the entire haplotype. For this to occur and for these *Rpv3* haplotypes to be so widespread in breeding germplasm, selection for resistance in many breeding schemes historically relied on phenotype over MAS. Regardless, there is a demonstrated need for updated marker technologies whose positions are refined in closer proximity to the potential causal genes. The use of higher resolution markers for MAS would also enable grapevines breeders to track recombination events within the locus and how that relates to changes in resistance efficacy and race-specificity, and would exchange the resources available for the fine mapping of causal alleles (Zou *et al.,* 2023). Core genome rhAmpSeq local haplotype markers typically have several hundred alleles across *Vitis* and could help to identify haplotype diversity missed by SSR analysis.

CONCLUSION

This study sought to characterize genome structural variation within the *Rpv3* and co-located *Rpv27* loci through the comparative studies of haplotype-resolved long-read genome assemblies. The alleles were categorized based on their diagnostic SSR markers and the copy numbers and locations of the validated *Rpv3.1* candidate genes were compared among alleles. Structural and sequence variation within and among allelic groups suggested the effect of selection on the locus and demonstrated the need for the development of new

markers that can distinguish each allele. In doing so, this work contributes to the knowledge of variation within *Rpv3* and lays the foundation for future work in understanding this complex resistance locus.

ACKNOWLEDGEMENTS

We would like to thank Gabriele Di Gaspero for providing valuable insights and critical review of this research prior to peer review. We would also like to thank the grape breeding programs who provided leaf samples for genome sequencing: Bruce Reisch for NY84.0101.03, Matt Clark for MN1264, and Chin-Feng Hwang for 'Norton'. An additional thank you to Erin Galarneau and the USDA National Plant Germplasm System for 'Catawba', 'Concord', and 'Horizon'. Funding was provided by the USDA Specialty Crop Research Initiative (Award No. 2022-51181-38240) and the USDA Agricultural Research Service (Project 8060-21220-008-000D).

REFERENCES

Arnold, C., Rossetto, M., McNally, J., and Henry, R. J. (2002). The application of SSRs characterized for grape (*Vitis vinifera*) to conservation studies in Vitaceae. *American Journal of Botany*, *89*(1), 22–28. https://doi.org/10.3732/ajb.89.1.22

Battilana, J., Lorenzi, S., Moreira, F. M., Moreno-Sanz, P., Failla, O., Emanuelli, F., and Grando, M. S. (2013). Linkage mapping and molecular diversity at the flower sex locus in wild and cultivated grapevine reveal a prominent SSR haplotype in hermaphrodite plants. *Molecular Biotechnology*, *54*(3), 1031–1037. https://doi.org/10.1007/s12033-013-9657-5

Bellin, D., Peressotti, E., Merdinoglu, D., Wiedemann-Merdinoglu, S., Adam-Blondon, A.-F., Cipriani, G., Morgante, M., Testolin, R., and Di Gaspero, G. (2009). Resistance to *Plasmopara viticola* in grapevine 'Bianca' is controlled by a major dominant gene causing localised necrosis at the infection site. *Theoretical and Applied Genetics*, *120*(1), 163–176. https://doi.org/10.1007/s00122-009-1167-2

Buchfink, B., Reuter, K., and Drost, H.-G. (2021). Sensitive protein alignments at tree-of-life scale using DIAMOND. *Nature Methods*, *18*(4), 366–368. https://doi.org/10.1038/s41592-021-01101-x

Bushnell, B. (2024). *BBMap: Short read aligner and other bioinformatic tools*. (Version 39.06) [Computer software]. https://sourceforge.net/projects/bbmap/

Cadle-Davidson, L. (2008). Variation within and between *Vitis* spp. for foliar resistance to the downy mildew pathogen *Plasmopara viticola*. *Plant Disease*, *92*(11), 1577–1584. https://doi.org/10.1094/PDIS-92-11-1577

Camacho, C., Coulouris, G., Avagyan, V., Ma, N., Papadopoulos, J., Bealer, K., and Madden, T. L. (2009). BLAST+: Architecture and applications. *BMC Bioinformatics*, *10*(1), 421. https://doi.org/10.1186/1471-2105-10-421

Casagrande, K., Falginella, L., Castellarin, S. D., Testolin, R., and Di Gaspero, G. (2011). Defence responses in *Rpv3*-dependent resistance to grapevine downy mildew. *Planta*, *234*(6), 1097–1109. https://doi.org/10.1007/s00425-011-1461-5

Charif, D., and Lobry, J. R. (2007). SeqinR 1.0-2: A contributed package to the R project for statistical computing devoted to biological sequences retrieval and analysis. In U. Bastolla, M. Porto, H. E. Roman, and M. Vendruscolo (Eds.), *Structural approaches to sequence evolution: Molecules, networks, populations* (pp. 207–232). Springer Verlag.

Cheng, H., Concepcion, G. T., Feng, X., Zhang, H., and Li, H. (2021). Haplotype-resolved de novo assembly using phased assembly graphs with hifiasm. *Nature Methods*, *18*(2), 170–175. https://doi.org/10.1038/s41592-020-01056-5

Clark, M. D., Teh, S. L., Burkness, E., Moreira, L., Watson, G., Yin, L., Hutchison, W. D., and Luby, J. J. (2018). Quantitative trait loci identified for foliar phylloxera resistance in a hybrid grape population. *Australian Journal of Grape and Wine Research*, *24*(3), 292–300. https://doi.org/10.1111/ajgw.12341

Delmotte, F., Mestre, P., Schneider, C., Kassemeyer, H.-H., Kozma, P., Richart-Cervera, S., Rouxel, M., and Delière, L. (2014). Rapid and multiregional adaptation to host partial resistance in a plant pathogenic oomycete: Evidence from European populations of *Plasmopara viticola*, the causal agent of grapevine downy mildew. *Infection, Genetics and Evolution*, *27*, 500–508. https://doi.org/10.1016/j.meegid.2013.10.017

Di Gaspero, G., Copetti, D., Coleman, C., Castellarin, S. D., Eibach, R., Kozma, P., Lacombe, T., Gambetta, G., Zvyagin, A., Cindrić, P., Kovács, L., Morgante, M., and Testolin, R. (2012). Selective sweep at the *Rpv3* locus during grapevine breeding for downy mildew resistance. *Theoretical and Applied Genetics*, *124*(2), 277–286. https://doi.org/10.1007/s00122-011-1703-8

Fischer, B. M., Salakhutdinov, I., Akkurt, M., Eibach, R., Edwards, K. J., Töpfer, R., and Zyprian, E. M. (2004). Quantitative trait locus analysis of fungal disease resistance factors on a molecular map of grapevine. *Theoretical and Applied Genetics*, *108*(3), 501–515. https://doi.org/10.1007/s00122-003-1445-3

Foria, S., Copetti, D., Eisenmann, B., Magris, G., Vidotto, M., Scalabrin, S., Testolin, R., Cipriani, G., Wiedemann-Merdinoglu, S., Bogs, J., Di Gaspero, G., and Morgante, M. (2020). Gene duplication and transposition of mobile elements drive evolution of the *Rpv3* resistance locus in grapevine. *The Plant Journal*, *101*(3), 529–542. https://doi.org/10.1111/tpj.14551

Foria, S., Magris, G., Morgante, M., and Di Gaspero, G. (2018). The genetic background modulates the intensity of *Rpv3*-dependent downy mildew resistance in grapevine. *Plant Breeding*, *137*(2), 220–228. https://doi.org/10.1111/pbr.12564

Gotz, S., Garcia-Gomez, J. M., Terol, J., Williams, T. D., Nagaraj, S. H., Nueda, M. J., Robles, M., Talon, M., Dopazo, J., and Conesa, A. (2008). High-throughput functional annotation and data mining with the Blast2GO suite. *Nucleic Acids Research*, *36*(10), 3420–3435. https://doi.org/10.1093/nar/gkn176

Grimaldi, M.-C., and Crouau-Roy, B. (1997). Microsatellite allelic homoplasy due to variable flanking sequences. *Journal of Molecular Evolution*, *44*(3), 336–340. https://doi.org/10.1007/PL00006151

Hammers, M., Sapkota, S., Chen, L.-L., and Hwang, C.-F. (2017). Constructing a genetic linkage map of *Vitis aestivalis*-derived "Norton" and its use in comparing Norton and Cynthiana. *Molecular Breeding*, *37*(5), 64. https://doi.org/10.1007/s11032-017-0644-6

Heyman, L., Höfle, R., Kicherer, A., Trapp, O., Ait Barka, E., Töpfer, R., and Höfte, M. (2021). The durability of quantitative host resistance and variability in pathogen virulence in the interaction between European grapevine cultivars and *Plasmopara viticola*. *Frontiers in Agronomy*, *3*, 684023. https://doi.org/10.3389/fagro.2021.684023

Hon, T., Mars, K., Young, G., Tsai, Y.-C., Karalius, J. W., Landolin, J. M., Maurer, N., Kudrna, D., Hardigan, M. A., Steiner, C. C., Knapp, S. J., Ware, D., Shapiro, B., Peluso, P., and Rank, D. R. (2020). Highly accurate long-read HiFi sequencing data for five complex genomes. *Scientific Data*, *7*(1), 399. https://doi.org/10.1038/s41597-020-00743-4

Koledenkova, K., Esmaeel, Q., Jacquard, C., Nowak, J., Clément, C., and Ait Barka, E. (2022). *Plasmopara viticola* the causal agent of downy mildew of grapevine: From its taxonomy to disease management. *Frontiers in Microbiology*, *13*, 889472. https://doi.org/10.3389/fmicb.2022.889472

Letunic, I., and Bork, P. (2021). Interactive Tree Of Life (iTOL) v5: An online tool for phylogenetic tree display and annotation. *Nucleic Acids Research*, *49*(W1), W293–W296. https://doi.org/10.1093/nar/gkab301

Marçais, G., Delcher, A. L., Phillippy, A. M., Coston, R., Salzberg, S. L., and Zimin, A. (2018). MUMmer4: A fast and versatile genome alignment system. *PLOS Computational Biology*, *14*(1), e1005944. https://doi.org/10.1371/journal.pcbi.1005944

Martin, E. C., Spiridon, L., Goverse, A., and Petrescu, A.-J. (2022). NLRexpress—A bundle of machine learning motif predictors—Reveals motif stability underlying plant nod-like receptors diversity. *Frontiers in Plant Science*, *13*, 975888. https://doi.org/10.3389/fpls.2022.975888

Massi, F., Torriani, S. F. F., Borghi, L., and Toffolatti, S. L. (2021). Fungicide resistance evolution and detection in plant pathogens: *Plasmopara viticola* as a case study. *Microorganisms*, *9*(1), 119. https://doi.org/10.3390/microorganisms9010119

Minio, A., Cochetel, N., Vondras, A. M., Massonnet, M., and Cantu, D. (2022). Assembly of complete diploid-phased chromosomes from draft genome sequences. *G3 Genes|Genomes|Genetics*, *12*(8), jkac143. https://doi.org/10.1093/g3journal/jkac143

Moshi. (2024). *pyGenomeViz* (v0.4.4) [Computer software]. https://github.com/moshi4/pyGenomeViz

Paineau, M., Mazet, I. D., Wiedemann-Merdinoglu, S., Fabre, F., and Delmotte, F. (2022). The characterization of pathotypes in grapevine downy mildew provides insights into the breakdown of *Rpv3*, *Rpv10*, and *Rpv12* factors in grapevines. *Phytopathology®*, *112*(11), 2329–2340. https://doi.org/10.1094/PHYTO-11-21-0458-R

Patel, S., Harris, Z. N., Londo, J. P., Miller, A., and Fennell, A. (2023). Genome assembly of the hybrid grapevine *Vitis* 'Chambourcin.' *Gigabyte*, *2023*, 1–18. https://doi.org/10.46471/gigabyte.84

Peng, J., Wang, X., Wang, H., Li, X., Zhang, Q., Wang, M., and Yan, J. (2024). Advances in understanding grapevine downy mildew: From pathogen infection to disease management. *Molecular Plant Pathology*, *25*(1), e13401. https://doi.org/10.1111/mpp.13401

R Core Team. (2023). *R: A language and environment for statistical computing*. https://www.R-project.org/

Reisch, B. (2024). *Grape varieties named at the New York State Agricultural Experiment Station Geneva, NY*. http://www.hort.cornell.edu/reisch/grapegenetics/nyreleases.html

Sapkota, S., Chen, L.-L., Yang, S., Hyma, K. E., Cadle-Davidson, L., and Hwang, C.-F. (2019). Construction of a high-density linkage map and QTL detection of downy mildew resistance in *Vitis aestivalis*-derived 'Norton.' *Theoretical and Applied Genetics*, *132*(1), 137–147. https://doi.org/10.1007/s00122-018-3203-6

Shi, X., Cao, S., Wang, X., Huang, S., Wang, Y., Liu, Z., Liu, W., Leng, X., Peng, Y., Wang, N., Wang, Y., Ma, Z., Xu, X., Zhang, F., Xue, H., Zhong, H., Wang, Y., Zhang, K., Velt, A., … Zhou, Y. (2023). The complete reference genome for grapevine (*Vitis vinifera* L.) genetics and breeding. *Horticulture Research*, *10*(5), uhad061. https://doi.org/10.1093/hr/uhad061

Stanke, M., Diekhans, M., Baertsch, R., and Haussler, D. (2008). Using native and syntenically mapped cDNA alignments to improve *de novo* gene finding. *Bioinformatics*, *24*(5), 637–644. https://doi.org/10.1093/bioinformatics/btn013

Steuernagel, B., Witek, K., Krattinger, S. G., Ramirez-Gonzalez, R. H., Schoonbeek, H., Yu, G., Baggs, E., Witek, A. I., Yadav, I., Krasileva, K. V., Jones, J. D. G., Uauy, C., Keller, B., Ridout, C. J., and Wulff, B. B. H. (2020). The NLR-Annotator tool enables annotation of the intracellular immune receptor repertoire. *Plant Physiology*, *183*(2), 468–482. https://doi.org/10.1104/pp.19.01273

Striem, J., Spiegel-Roy, P., Ben-Hayyim, G., Beckmann, J., and Gidoni, D. (1990). Genomic DNA fingerprinting of *Vitis vinifera* by the use of multi-loci probes. *Vitis*, *29*, 223–227.

Tamura, K., Stecher, G., and Kumar, S. (2021). MEGA11: Molecular evolutionary genetics analysis version 11. *Molecular Biology and Evolution*, *38*(7), 3022–3027. https://doi.org/10.1093/molbev/msab120

Velt, A., Frommer, B., Blanc, S., Holtgräwe, D., Duchêne, É., Dumas, V., Grimplet, J., Hugueney, P., Kim, C., Lahaye, M., Matus, J. T., Navarro-Payá, D., Orduña, L., Tello-Ruiz, M. K., Vitulo, N., Ware, D., and Rustenholz, C. (2023). An improved reference of the grapevine genome reasserts the origin of the PN40024 highly homozygous genotype. *G3: Genes, Genomes, Genetics*, *13*(5), jkad067. https://doi.org/10.1093/g3journal/jkad067

Vezzulli, S., Malacarne, G., Masuero, D., Vecchione, A., Dolzani, C., Goremykin, V., Mehari, Z. H., Banchi, E., Velasco, R., Stefanini, M., Vrhovsek, U., Zulini, L., Franceschi, P., and Moser, C. (2019). The *Rpv3-3* haplotype and stilbenoid induction mediate downy mildew resistance in a grapevine interspecific population. *Frontiers in Plant Science*, *10*, 234. https://doi.org/10.3389/fpls.2019.00234

Wairich, A., Malabarba, J., Buffon, V., Porto, D. D., Togawa, R., and Revers, L. F. (2022). Molecular characterization of the *Rpv3* locus towards the development of KASP markers for downy mildew resistance in grapevine (*Vitis* spp.). *Euphytica*, *218*(1), 5. https://doi.org/10.1007/s10681-021-02952-3

Welter, L. J., Göktürk-Baydar, N., Akkurt, M., Maul, E., Eibach, R., Töpfer, R., and Zyprian, E. M. (2007). Genetic mapping and localization of quantitative trait loci affecting fungal disease resistance and leaf morphology in grapevine (*Vitis vinifera* L). *Molecular Breeding*, *20*(4), 359–374. https://doi.org/10.1007/s11032-007-9097-7

Zou, C., Karn, A., Reisch, B., Nguyen, A., Sun, Y., Bao, Y., Campbell, M. S., Church, D., Williams, S., Xu, X., Ledbetter, C. A., Patel, S., Fennell, A., Glaubitz, J. C., Clark, M., Ware, D., Londo, J. P., Sun, Q., and Cadle-Davidson, L. (2020). Haplotyping the *Vitis* collinear core genome with rhAmpSeq improves marker transferability in a diverse genus. *Nature Communications*, *11*(1), 413. https://doi.org/10.1038/s41467-019-14280-1

Zou, C., Sapkota, S., Figueroa-Balderas, R., Glaubitz, J., Cantu, D., Kingham, B. F., Sun, Q., and Cadle-Davidson, L. (2023). A multitiered haplotype strategy to enhance phased assembly and fine mapping of a disease resistance locus. *Plant Physiology*, *193*(4), 2321–2336. https://doi.org/10.1093/plphys/kiad494

Zyprian, E., Ochßner, I., Schwander, F., Šimon, S., Hausmann, L., Bonow-Rex, M., Moreno-Sanz, P., Grando, M. S., Wiedemann-Merdinoglu, S., Merdinoglu, D., Eibach, R., and Töpfer, R. (2016). Quantitative trait loci affecting pathogen resistance and ripening of grapevines. *Molecular Genetics and Genomics*, *291*(4), 1573–1594. https://doi.org/10.1007/s00438-016-1200-5